Author Manuscript
Accepted for publication in a peer-reviewed journal

NIST National Institute of Standards and Technology • U.S. Department of Commerce

Published in final edited form as:
IEEE Trans Power Syst. 2018 ; 33: . doi:10.1109/TPWRS.2018.2801121.

MMSE-based analytical estimator for uncertain power system with limited number of measurements

Hasnae Bilil, Member, IEEE and **Hamid Gharavi, Life Fellow, IEEE**
Advanced Network Technologies Division, National Institute of Standards and Technology, MD, USA

Abstract

The expected penetration of a large number of renewable distributed energy resources (DER's) is driving next generation power systems toward uncertainties that can have a huge impact on the reliability and complexities of state estimation. Therefore, the stochastic power flow (SPF) and forecasting-aided state estimation of power systems integrating DER's are becoming a major challenge for operation of the future grid. In this paper we propose a new state estimation method referred to as 'mean squared estimator' (MSE) to deal with the uncertain nature of the power system parameters. The estimator benefits from the prior study of SPF, which involves the probability density functions (PDF's) of the system parameters. The main advantage of this estimator is based on its ability to instantaneously incorporate the dynamics of the power system. Moreover, the analytical formula of MSE expresses the mean value of the estimated parameters corrected by an additional term that takes into account the measurement of the parameters. It is shown that the proposed MSE can provide an accurate state estimation with a limited number of measurements with guaranteed convergence. MSE has been tested using IEEE 14, 30, 39 and 118 bus models for different measurement redundancies. The results have been compared to methods such as weighted least square (WLS), unscented Kalman filter (UKF) and compressive sensing-based UKF (CS-UKF). The numerical results show superior performances, especially under a limited number of measurements where WLS and UKF may lead to divergence.

Index Terms

Dynamic state estimation; minimum mean-squared error; Gaussian mixture model; analytic estimator; limited number of measurements

I. Introduction

The deployment of renewable resources in distributed grid systems poses a set of new challenges mainly due to their variability and dependency on climate parameters, which can have a major impact on the system parameters that are needed to measure power flow and state estimation. The first aims at calculating the entire system parameters, based on prior knowledge (or prediction) of some of the parameters, while the latter, which is the backbone of energy management systems, estimates these parameters measured under noisy conditions. More precisely, a state estimator aims at providing estimated values of the

system parameters roughly equal to the true values by eliminating measurement errors. In the presence of renewables, many studies in the past have incorporated the system uncertainties for power flow measurement and state estimation. Stochastic power flow (SPF) and forecast-aided state estimation, also called dynamic state estimation (DSE), take into consideration the uncertain behavior of power generations and loads. The main objective is to determine the probability density function (PDF) of the power system parameters to solve the SPF problem [1]–[13]. For instance, in [1], the authors propose to combine the concept of Cumulants and Gram-Charlier's expansion theory, and [2] presents a comparative and analytic study of four different Hong's point estimate schemes to solve the SPF problem. A practical method to tackle various random variables, such as renewable energy sources parameters that follow different types of probability distributions, has also been proposed in [4]. In the case of unknown input PDF's, a method for nonparametric probabilistic load flow analysis is developed in [5]. Other studies mainly use a Gaussian mixture model (GMM) to approximate the PDF of loads or a mix of DER's, which cannot be approximated with a known shape PDF [6]–[8]. Furthermore, there has been tremendous effort towards real-time DSE in support of next generation power systems [14]–[23]. In particular, with the emergence of the phasor measurement units (PMU's) having the unique capability of providing synchronous measurements, real-time DSE has been receiving considerable attention [24]–[36]. Moreover, various versions of Kalman filtering have also been developed in order to improve DSE performances and its robustness while reducing the execution time [33], [34]. For instance, three versions of Kalman filtering, namely, extended Kalman filter (EKF), the unscented Kalman filter (UKF), and the Cubature Kalman filter (CKF) with or without PMU's measurements have been evaluated in [35]. By utilizing the PMU's measurements, the authors in [36] have developed an extended Kalman filter with unknown inputs (EKF-UI) that can estimate the states as well as the unknown inputs of the synchronous machine. On the other hand, the study in [22] describes a generalized maximum likelihood (GM)-estimator on power systems (GM-PSE). In this method, short-term forecasts of the distributed energy resources (DER's) and loads are first calculated to predict the states. A redundant batch regression model is then used to process the predicted states and measured parameters. The method uses an iteratively re-weighted least squares (IRLS) algorithm to obtain the final estimated states. To track the system transients faster and with better reliability, the same authors present an iterated extended Kalman filter using the generalized maximum likelihood approach (termed GM-IEKF) [23]. We should point out, however, that all aforementioned methods are designed to predict and then estimate the states regardless of any prior knowledge of the states PDF's that the SPF is supposed to determine.

In this paper, we present a new analytic-based state estimator, referred to as 'Mean Square Estimator' (MSE), that uses the outputs of the SPF by assuming a prior knowledge of the state parameters distribution regardless of their shapes. Specifically, our approach is based on the calculus of the minimum mean squared error (MMSE) that deals with generally non-Gaussian Random Variables (NGRV's). Therefore, the GMM, which is an approximate presentation of the PDF's of NGRV's, is utilized in the proposed estimator. As a weighted sum of several Gaussian components, GMM is widely used for NGRVs probability distribution [6]–[8], [37], [38]. More specifically, in many studies, GMM has been suggested

to model the PDFs of load power and renewable energy sources [39]–[43]. Since the proposed MMSE-based estimator is an analytical approach, it can provide estimated values instantaneously. In addition, its performance remains good even with a limited number of measurements, which is important in the case of a wide system. For instance, an extension of state estimation to medium and low voltage grids may require a large number of measurements that can have a considerable impact on state estimation complexities. In terms of performance, the proposed estimator is compared with the weighted least squares method (WLS) and UKF using various IEEE test systems.

The paper is organized as follows: Section II presents the fundamentals of GMM presentation of NGRV's. Section III introduces the formulation of the proposed MSE as a conditional expectation of the estimated states for the given measurements. Section IV derives formulas of generating moments followed by the general formula of MSE when states and measurements are NGRV's. The results of the proposed state estimation approach using the IEEE 14, 30 and 118 bus models are then presented in Section VI. Finally, Section VII provides the conclusion and some perspectives.

II. Gaussian Mixture model

In this section we give a brief overview of the fundamentals of GMM for the presentation of any NGRV as a function of Gaussian components. Gaussian distribution, which is commonly used for modeling univariate data, can be extended to two or more variables. There are many studies in open literature that provide the formulation of any order of the moments of Gaussian random variables (GRVs) [41], [42]. Furthermore, Gaussian distribution can be considered to formulate the moments of NGRVs. Note that in the rest of the paper, the notations IE($\boldsymbol{X}$), $\boldsymbol{X}^{\mathrm{T}}$ and $\boldsymbol{X}^{-1}$ are used to express the expectation, the transposed and inverse matrices of $\boldsymbol{X}$ respectively.

A. Gaussian Density

A multivariate random variable $\boldsymbol{x} = [x_1, x_2, \ldots, x_n]$ is said to be distributed as the multivariate Gaussian distribution with mean $\boldsymbol{\mu_x}$ and covariance matrix $\boldsymbol{\Sigma_x}$, $\boldsymbol{x} \sim \mathcal{N}(\boldsymbol{x};\boldsymbol{\mu_x},\boldsymbol{\Sigma_x})$, if the density function of $\boldsymbol{x}$ is given by [44]

$$g(\boldsymbol{x} \mid \boldsymbol{\mu_x}, \boldsymbol{\Sigma_x}) = \frac{1}{\sqrt{(2\pi)^n \mid \boldsymbol{\Sigma_x} \mid}} \ldots \exp\left[-\frac{1}{2}\left((\boldsymbol{x}-\boldsymbol{\mu_x})^T \boldsymbol{\Sigma_x}^{-1}(\boldsymbol{x}-\boldsymbol{\mu_x})\right)\right] \quad (1)$$

B. Gaussian Mixture Model

The Gaussian Mixture Model (GMM) is an approximate presentation of a non-Gaussian density function of a random variable $\boldsymbol{x}$ (it can be a multivariate variable) by a mixture (a summation) of $L_{\boldsymbol{x}}$ Gaussian distribution components [6]–[8], [37], [38]. It can be expressed as,

$$f_X(\boldsymbol{x}) = \sum_{i=1}^{L_{\boldsymbol{x}}} w_{\boldsymbol{x}\mid i} g(\boldsymbol{x} \mid \boldsymbol{\mu}_{\boldsymbol{x}\mid i}, \boldsymbol{\Sigma}_{\boldsymbol{x}\mid i}), \quad (2)$$

where $\boldsymbol{x}$ is an n-dimensional vector of continuous values, the vector of the estimation problem parameters, w_i, $i = 1, \ldots, L_{\boldsymbol{x}}$, are the mixture weights, and $g(\boldsymbol{x}|\boldsymbol{\mu}_{\boldsymbol{x}|i}, \boldsymbol{\Sigma}_{\boldsymbol{x}|i})$, $i = 1, \ldots, L_{\boldsymbol{x}}$, are the components Gaussian densities. Each component is an n–variate Gaussian function as defined preciously, with $\boldsymbol{\mu}_{\boldsymbol{x}|i}$ and $\boldsymbol{\Sigma}_{\boldsymbol{x}|i}$ being the mean vector and the covariance matrix of $\boldsymbol{x}$, respectively. The mixture weights satisfy the following equality,

$$\sum_{i=1}^{L_{\boldsymbol{x}}} w_{\boldsymbol{x}\mid i} = 1, \quad (3)$$

Therefore, the mean value vector and covariance matrix of $\boldsymbol{x}$ can be approximated in terms of the Gaussian components parameters as follows,

$$\boldsymbol{\mu}_{\boldsymbol{x}} = \sum_{i=1}^{L_{\boldsymbol{x}}} w_{\boldsymbol{x}\mid i} \boldsymbol{\mu}_{\boldsymbol{x}\mid i}, \quad (4)$$

$$\boldsymbol{\Sigma}_{\boldsymbol{x}} = \sum_{i=1}^{L_{\boldsymbol{x}}} w_{\boldsymbol{x}\mid i} \left(\boldsymbol{\Sigma}_{\boldsymbol{x}\mid i} + \left(\boldsymbol{\mu}_{\boldsymbol{x}\mid i} - \boldsymbol{\mu}_{\boldsymbol{x}} \right) \left(\boldsymbol{\mu}_{\boldsymbol{x}\mid i} - \boldsymbol{\mu}_{\boldsymbol{x}} \right)^{\mathrm{T}} \right). \quad (5)$$

III. Minimum mean square error based power system state estimation

A. Problem formulation

State estimation aims at determining an optimal estimation of a vectors' parameters $\boldsymbol{x} = [x_1, \ldots, x_N]$ giving a vector of measurements $\boldsymbol{z} = [z_1, \ldots, z_M]$ and functions $\boldsymbol{h} = [h_1, \ldots, h_M]$] based on the following relationship,

$$\boldsymbol{z} = \boldsymbol{h}(\boldsymbol{x}) + \boldsymbol{v} \quad (6)$$

where $\boldsymbol{v}$ represents the noise. In the case of power system state estimation, the estimated parameters are voltage amplitudes and angles, e.g. $\boldsymbol{x} = [\boldsymbol{\theta}, \boldsymbol{V}]$. Moreover, using PMU's or Supervisory Control And Data Acquisition (SCADA) measurements, the function $h_j(\boldsymbol{x})$ is either a linear function of voltage amplitude and angle measurements or a non-linear function of active and reactive power measurements. Notations $\mathscr{I}_V, \mathscr{I}_\theta, \mathscr{I}_P, \mathscr{I}_Q$ stand for

the sets of buses equipped with measurements meters of voltage amplitude and angles, active and reactive power injections respectively. $\mathscr{Z}_{P_f}$ and $\mathscr{Z}_{Q_f}$ present the sets of pairs of buses with measured active and reactive power flow respectively. Therefore,

$$\begin{cases} h_j(\boldsymbol{x}) = V_n & \text{for } z_j = z_{V_n},\ n \in \mathscr{Z}_V \\ h_j(\boldsymbol{x}) = \theta_n & \text{for } z_j = z_{\theta_n},\ n \in \mathscr{Z}_\theta \\ h_j(\boldsymbol{x}) = P_n & \text{for } z_j = z_{P_n},\ n \in \mathscr{Z}_P \\ h_j(\boldsymbol{x}) = Q_n & \text{for } z_j = z_{Q_n},\ n \in \mathscr{Z}_Q \\ h_j(\boldsymbol{x}) = P_{nk} & \text{for } z_j = z_{P_{nk}},\ (n,k) \in \mathscr{Z}_{P_f} \\ h_j(\boldsymbol{x}) = Q_{nk} & \text{for } z_j = z_{Q_{nk}},\ (n,k) \in \mathscr{Z}_{Q_f} \end{cases} \quad j = 1, \ldots, M \qquad (7)$$

In the above, z_{V_n}, z_{θ_n} are the measurement values of voltage amplitude and angle, respectively at bus n and z_{P_n}, z_{Q_n} are the measurements of active and reactive power: P_n, Q_n, defined in (8), (9) respectively, and $z_{P_{nk}}$, $z_{Q_{nk}}$ correspond to the measurements of active and reactive power flow P_{nk}, Q_{nk} between the buses n and k, as defined in (10), (11) respectively [45].

$$P_n = V_n \sum_{k \in \mathscr{N}} V_k (G_{nk} \cos\theta_{nk} + B_{nk} \sin\theta_{nk}) \qquad (8)$$

$$Q_n = V_n \sum_{k \in \mathscr{N}} V_k (G_{nk} \sin\theta_{nk} - B_{nk} \cos\theta_{nk}) \qquad (9)$$

$$P_{nk} = -V_n^2 G_{nk} + V_n V_k (G_{nk} \cos\theta_{nk} + B_{nk} \sin\theta_{nk}) \qquad (10)$$

$$Q_{nk} = -V_n^2 B_{nk} - V_n V_m (G_{nk} \sin\theta_{nk} - B_{nk} \cos\theta_{nk}) \qquad (11)$$

where the notation V_n stands for the voltage magnitude at the n^{th} bus. $\theta_{nk} = \theta_n - \theta_k$ is the angular difference of voltage phases at the buses n and k, G_{nk} and B_{nk} are the real and imaginary part of admittance elements. $\mathscr{N}$ is the set of the network buses.

B. Minimum mean-squared error

The objective function of an MMSE-based estimator is defined as follows [44],

$$\min_{\hat{\boldsymbol{x}}_{\mathrm{MS}}} J(\tilde{\boldsymbol{x}}_{\mathrm{MS}}) \quad (12)$$

with

$$J(\tilde{\boldsymbol{x}}_{\mathrm{MS}}) = \mathrm{IE}\,(\tilde{\boldsymbol{x}}_{\mathrm{MS}}^{\mathrm{T}}\tilde{\boldsymbol{x}}_{\mathrm{MS}})$$

where $\tilde{\boldsymbol{x}}_{\mathrm{MS}} = \boldsymbol{x} - \hat{\boldsymbol{x}}_{\mathrm{MS}}$ is the estimation error of $\boldsymbol{x}$ and $\hat{\boldsymbol{x}}_{\mathrm{MS}}$ is the estimated value of $\boldsymbol{x}$ using MSE. $\tilde{\boldsymbol{x}}_{\mathrm{MS}}^{\mathrm{T}}$ is the transposed vector of $\tilde{\boldsymbol{x}}_{\mathrm{MS}}$. The solution to this problem, as proven in [44] is the conditional expectation of $\boldsymbol{x}$ knowing the measurements vector z,

$$\hat{\boldsymbol{x}}_{\mathrm{MS}} = \mathrm{IE}(\boldsymbol{x} \mid z), \quad (13)$$

This result is called the fundamental theorem of estimation theory and is true for both linear and non-linear system [44]. Moreover, the minimum value of $J(\tilde{\boldsymbol{x}}_{\mathrm{MS}})$, which also presents the variance of the estimation error, is given as,

$$J^{*}(\tilde{\boldsymbol{x}}_{\mathrm{MS}}) = \mathrm{IE}(\boldsymbol{x}^{\mathrm{T}}\boldsymbol{x} \mid z) - \mathrm{IE}(\boldsymbol{x}^{\mathrm{T}} \mid z)\mathrm{IE}(\boldsymbol{x} \mid z)\,. \quad (14)$$

where $\boldsymbol{x}^{\mathrm{T}}$ is the transposed vector of $\boldsymbol{x}$. This expression is the summation of the conditional variances of the elements of $\boldsymbol{x}$ knowing z.

C. Mean squared estimator for Gaussian input parameters

According to [44], when $\boldsymbol{x}$ and z are jointly Gaussian, the estimator that minimizes the mean-squared error is

$$\hat{\boldsymbol{x}}_{\mathrm{MS}} = \boldsymbol{\mu}_{\boldsymbol{x}} + \boldsymbol{\Sigma}_{xz}\boldsymbol{\Sigma}_{z}^{-1}[z - \boldsymbol{\mu}_{z}]\,. \quad (15)$$

Furthermore, the above estimator for $\boldsymbol{x}$ is NGRV's can be expressed in two forms depending on z is Gaussian or non-Gaussian. Nonetheless, the estimator given in (15) provides an optimal state estimation which would require determining the value of the covariance matrix $\boldsymbol{\Sigma}_{xz}$ of the estimated parameters and the measurements, as well as the covariance matrix $\boldsymbol{\Sigma}_{z}$ of the measurements. Elements $\Sigma_{x_i z_j}$ for the elements $(i, j) \in \mathcal{N}_{\mathrm{s}} \times \mathcal{N}_{\mathrm{m}}$ ($\mathcal{N}_{\mathrm{s}}$, $\mathcal{N}_{\mathrm{m}}$ are the sets of estimated parameters and measurements respectively) in the matrix $\boldsymbol{\Sigma}_{xz}$ can be calculated using the following expression of two RV's covariance,

$$\sum_{x_i z_j} = \mathrm{IE}(x_i z_j) - \mu_{x_i} \mu_{z_j}, \quad (16)$$

From (6),

$$z_j = h_j(\boldsymbol{x}) + v_j.$$

Therefore,

$$\mathrm{IE}(x_i z_j) = \mathrm{IE}(x_i h_j(\boldsymbol{x})) + \mathrm{IE}(x_i v_j), \quad (17)$$

Consider x_i and v_j uncorrelated, then $\mathrm{IE}(x_i v_j) = \mathrm{IE}(x_i)\mathrm{IE}(v_j)$. Assuming that the noise has zero mean $\mathrm{IE}(v_j) = 0$, the following expression can be obtained,

$$\mathrm{IE}(x_i z_j) = \mathrm{IE}(x_i h_j(\boldsymbol{x})). \quad (18)$$

This clearly indicates that computation of matrix $\boldsymbol{\Sigma_{xz}}$ would require calculating the expectation values $\mathrm{IE}(x_i h_j(\boldsymbol{x}))$. This matrix can be expressed in terms of sub-matrices that correspond to covariances between the estimated state parameters and the measurements as given in (7). Therefore, $\boldsymbol{\Sigma_{xz}}$ can be expressed as,

$$\boldsymbol{\Sigma_{xz}} = \begin{bmatrix} \boldsymbol{\Sigma_{\theta,\theta}} & \boldsymbol{\Sigma_{\theta,V}} & \boldsymbol{\Sigma_{\theta,P}} & \boldsymbol{\Sigma_{\theta,Q}} & \boldsymbol{\Sigma_{\theta,P_f}} & \boldsymbol{\Sigma_{\theta,Q_f}} \\ \boldsymbol{\Sigma_{V,\theta}} & \boldsymbol{\Sigma_{V,V}} & \boldsymbol{\Sigma_{V,P}} & \boldsymbol{\Sigma_{V,Q}} & \boldsymbol{\Sigma_{V,P_f}} & \boldsymbol{\Sigma_{V,Q_f}} \end{bmatrix} \quad (19)$$

where $\boldsymbol{\Sigma_{\theta,\theta}}$, $\boldsymbol{\Sigma_{\theta,V}}$, $\boldsymbol{\Sigma_{\theta,P}}$, $\boldsymbol{\Sigma_{\theta,Q}}$, $\boldsymbol{\Sigma_{\theta,P_f}}$, $\boldsymbol{\Sigma_{\theta,Q_f}}$ are the covariance matrices between the voltage angle (estimated parameter) and the measurement parameters, i.e. voltage angle and amplitude, power injections and power flows, respectively. While $\boldsymbol{\Sigma_{V,\theta}}$, $\boldsymbol{\Sigma_{V,V}}$, $\boldsymbol{\Sigma_{V,P}}$, $\boldsymbol{\Sigma_{V,Q}}$, $\boldsymbol{\Sigma_{V,P_f}}$, $\boldsymbol{\Sigma_{V,Q_f}}$ hold the covariance matrices between the voltage amplitude (estimated parameter) and the measurement parameters, i.e. voltage angle and amplitude, power injections and power flows, respectively.

The calculus of the mean values $\mathrm{IE}(x_i z_j)$ can be achieved using the PDF's of voltage and measurement parameters, given by the SPF study. In the same way, the elements of the measurements covariance matrix $\boldsymbol{\Sigma_z}$ can be expressed as the difference between the mean value of the product of two measurements and the product of their mean values.

IV. General formula of mean squared estimator

Monitoring and state estimation of power system parameters requires the treatment of several NGRV's. For theoretical reasons, assume a Gaussian distribution of uncertain variables can be most conveniently used for state estimation [44], [46]. The purpose behind this section is to present the general formula of MSE by developing the calculus of IE($\boldsymbol{x}|\boldsymbol{z}$) in the case where states and measurements are NGRV's. To achieve this, we develop the calculus of the moments of a generic set of NGRV's, which are based on the GMM approximation of these variables.

A. On the moments of correlated non-Gaussian random variables

As mentioned before, the MMSE-based estimator is formulated in terms of the moments of voltage parameters, e.g. amplitudes and angles, and measurements. The PDF's of these parameters are not generally Gaussian. Therefore, based on the GMM approximation of these parameters, an analytical solution of the moments of NGRV's is developed in the following using formulas of the moments of GRV's.

Proposition 1 (Moments of NGRV)—Let $\boldsymbol{x}$ be a RV and its GMM is as given in (2). Therefore,

$$\mathrm{IE}(x_1 x_2 \ldots x_n) = \sum_{i=1}^{L_{\boldsymbol{x}}} \omega_{\boldsymbol{x}\,|\,i} \mathrm{IE}(x_1 x_2 \ldots x_n \mid \boldsymbol{\mu}_{\boldsymbol{x}\,|\,i}, \boldsymbol{\Sigma}_{\boldsymbol{x}\,|\,i}), \quad (20)$$

where IE($x_1 x_2 \ldots x_n|\boldsymbol{\mu}_{\boldsymbol{x}|i}, \boldsymbol{\Sigma}_{\boldsymbol{x}|i}$) is the moments of $x_1, x_2, \ldots, x_n$ based on the i^{th} component of $\boldsymbol{x}$'s PDF.

Proof: Consider the characteristic function of $\boldsymbol{x}$ as,

$$\begin{aligned} \varphi_{\boldsymbol{x}}(\boldsymbol{u}) &= \int_{\mathrm{IR}^n} \exp\{j(\boldsymbol{u}, \boldsymbol{x})\} f_{\boldsymbol{X}}(\boldsymbol{x}) dx \quad (21) \\ &= \sum_{i=1}^{L_x} \omega_{\boldsymbol{x}\,|\,i} \int_{\mathrm{IR}^n} \exp\{j(\boldsymbol{u}, \boldsymbol{x})\} g(\boldsymbol{x} \mid \boldsymbol{\mu}_{\boldsymbol{x}\,|\,i}, \boldsymbol{\Sigma}_{\boldsymbol{x}\,|\,i}) dx \\ &= \sum_{i=1}^{L_x} \omega_{\boldsymbol{x}\,|\,i} \varphi_{\boldsymbol{x}\,|\,i}(\boldsymbol{u}) \end{aligned}$$

where $\boldsymbol{\varphi}_{\boldsymbol{x}|\boldsymbol{i}}$ is the characteristic function of a jointly Gaussian random variable. j is the complex number defined as $j^2 = -1$ and $(\boldsymbol{u}, \boldsymbol{x})$ denotes the scalar product of $\boldsymbol{u}$ and $\boldsymbol{x}$, i.e. $(\boldsymbol{u}, \boldsymbol{x}) = \boldsymbol{u}^T \boldsymbol{x}$. Given that the moments of n random variables can be obtained by differentiating the characteristic function,

$$\mathrm{IE}(x_1 x_2 \ldots x_n) = \frac{1}{j^n} \frac{\partial^n}{\partial u_1 \ldots \partial u_n} \varphi_{\boldsymbol{x}}(\boldsymbol{u}) \mid_{\boldsymbol{u}=0} \quad (22)$$

Using the expression in (21), the moment of n NGRV's can be obtained as,

$$\mathrm{IE}(x_1 x_2 \ldots x_n) = \sum_{i=1}^{L_{\boldsymbol{x}}} \omega_{\boldsymbol{x}\mid i} \frac{1}{j^n} \frac{\partial^n}{\partial u_1 \ldots \partial u_n} \varphi_{\boldsymbol{x}\mid i}(\boldsymbol{u}) \mid_{\boldsymbol{u}=0} \quad (23)$$

Therefore, the expression of the moment of NGRV's can be given in terms of the moments of the Gaussian components in GMM of these RV's, as expressed in (20).

B. General formula of MSE

The MMSE-based estimator presented in (15) is optimal when the states are GRV. Generally the voltage amplitude and angle are non-Gaussian. A new formula of the MSE estimator is presented in the following proposition for an NGRV for $\boldsymbol{x}$, when GMM components of $\boldsymbol{x}$ and z are jointly Gaussian.

Proposition 2 (Conditional expectation of NGRV)—Let $\boldsymbol{x}$ be an NGRV whose GMM is given in (2) and z being a GRV. If each of the GMM components of $\boldsymbol{x}$ and z are jointly then,

$$\mathrm{IE}(\boldsymbol{x} \mid z) = \boldsymbol{\mu}_{\boldsymbol{x}} + \sum_{i=1}^{L_{\boldsymbol{x}}} \omega_{\boldsymbol{x}\mid i} \boldsymbol{\Sigma}_{\boldsymbol{x}\mid i,z} \boldsymbol{\Sigma}_z^{-1} [z - \boldsymbol{\mu}_z]. \quad (24)$$

with $\boldsymbol{\Sigma}_{\boldsymbol{x}|i,z}$ is the covariance matrix of $\boldsymbol{x}$ (i.e., the i^{th} components of its GMM) and z.

Proof: Applying Proposition 1 in the case of the first moment,

$$\mathrm{IE}(\boldsymbol{x} \mid z) = \sum_{i=1}^{L_{\boldsymbol{x}}} \omega_{\boldsymbol{x}\mid i} \mathrm{IE}(\boldsymbol{x} \mid z, \boldsymbol{\mu}_{\boldsymbol{x}\mid i}, \boldsymbol{\Sigma}_{\boldsymbol{x}\mid i}), \quad (25)$$

where $\mathrm{IE}(\boldsymbol{x}|z,\boldsymbol{\mu}_{\boldsymbol{x}|i},\boldsymbol{\Sigma}_{\boldsymbol{x}|i})$ is the expectation of $\boldsymbol{x}$ following the i^{th} Gaussian component of GMM of $\boldsymbol{x}$'s PDF, conditioned by z. Thus, we can show,

$$\mathrm{IE}(\boldsymbol{x} \mid z, \boldsymbol{\mu}_{\boldsymbol{x}\mid i}, \boldsymbol{\Sigma}_{\boldsymbol{x}\mid i}) = \mu_{\boldsymbol{x}\mid i} + \boldsymbol{\Sigma}_{\boldsymbol{x}\mid i,z} \boldsymbol{\Sigma}_z^{-1} [z - \boldsymbol{\mu}_z]. \quad (26)$$

Giving that,

$$\sum_{i=1}^{L_{\boldsymbol{x}}} \omega_{\boldsymbol{x}\mid i}\boldsymbol{\mu}_{\boldsymbol{x}\mid i} = \boldsymbol{\mu}_{\boldsymbol{x}}$$

This indicates that IE($\boldsymbol{x}|\boldsymbol{z}$) can indeed be expressed as in (24). However, we should emphasize that proposition 2 provides the formula of conditional expectation when the general expected parameter (NGRV) is conditioned by a GRV. However, measurements in a power system, i.e. voltage parameters (amplitude and angle), power injection, and power flow can also be NGRV. Later, we present the calculus of the conditional expectation of NGRV conditioned by NGRV.

Proposition 3 (Expectation of NGRV conditioned by NGRV)—Let $\boldsymbol{x}$ and $\boldsymbol{z}$ be NGRV's whose PDF's are approximated by GMM according to (2) and (27), respectively,

$$f_{\boldsymbol{Z}}(z) = \sum_{j=1}^{L_z} \omega_{z\mid j} g(z \mid \boldsymbol{\mu}_{z\mid j}, \boldsymbol{\Sigma}_{z\mid j}), \quad (27)$$

then

$$\mathrm{IE}(\boldsymbol{x} \mid z) = \boldsymbol{\mu}_{\boldsymbol{x}} + \sum_{i=1}^{L_{\boldsymbol{x}}} \sum_{j=1}^{L_z} \omega_{\boldsymbol{x}\mid i}\omega_{z\mid i} A_{\boldsymbol{x}\mid i,z\mid j}\left[z - \boldsymbol{\mu}_{z\mid j}\right]. \quad (28)$$

with

$$A_{\boldsymbol{x}\mid i,z\mid j} = \frac{g(z \mid \boldsymbol{\mu}_{z\mid j}, \boldsymbol{\Sigma}_{z\mid j})}{f_{\boldsymbol{Z}}(z)} \boldsymbol{\Sigma}_{\boldsymbol{x}\mid i,z\mid j} \boldsymbol{\Sigma}_{z\mid j}^{-1}. \quad (29)$$

where $\boldsymbol{\Sigma}_{\boldsymbol{x}|i,z|j}$ is the covariance matrix of $\boldsymbol{x}$ and $\boldsymbol{z}$ based on the i^{th} and j^{th} components of their GMM's.

Proof: To prove this proposition, we use the conditional density function as defined in [44], [47], expressed as

$$f_{\boldsymbol{X}\mid \boldsymbol{Z}}(\boldsymbol{x} \mid z) = \frac{f_{\boldsymbol{X},\boldsymbol{Z}}(\boldsymbol{x}, z)}{f_{\boldsymbol{Z}}(z)}. \quad (30)$$

Now let $\boldsymbol{y} = \begin{bmatrix} \boldsymbol{x} \\ \boldsymbol{z} \end{bmatrix}, \boldsymbol{\mu}_{\boldsymbol{y} \mid i,j} = \begin{bmatrix} \boldsymbol{\mu}_{\boldsymbol{x} \mid i} \\ \boldsymbol{\mu}_{\boldsymbol{z} \mid j} \end{bmatrix}$ and

$$\boldsymbol{\Sigma}_{\boldsymbol{y} \mid i,j} = \begin{bmatrix} \boldsymbol{\Sigma}_{\boldsymbol{x} \mid i} & \boldsymbol{\Sigma}_{\boldsymbol{x} \mid i,\boldsymbol{z} \mid j} \\ \boldsymbol{\Sigma}_{\boldsymbol{z} \mid j,\boldsymbol{x} \mid i} & \boldsymbol{\Sigma}_{\boldsymbol{z} \mid j} \end{bmatrix}$$

Herein, the joint PDF of x and z is approximated as follows,

$$f_{\boldsymbol{X},\boldsymbol{Z}}(\boldsymbol{x},\boldsymbol{z}) = \sum_{i=1}^{L_{\boldsymbol{x}}} \sum_{j=1}^{L_{\boldsymbol{z}}} \omega_{\boldsymbol{x} \mid i} \omega_{\boldsymbol{z} \mid j} g(\boldsymbol{y} \mid \boldsymbol{\mu}_{\boldsymbol{y} \mid i,j}, \boldsymbol{\Sigma}_{\boldsymbol{y} \mid i,j}), \quad (31)$$

Therefore,

$$f_{\boldsymbol{X},\boldsymbol{Z}}(\boldsymbol{x},\boldsymbol{z}) = \sum_{j=1}^{L_{\boldsymbol{z}}} \omega_{\boldsymbol{z} \mid j} f_{\boldsymbol{X},\boldsymbol{Z}}(\boldsymbol{x},\boldsymbol{z} \mid \boldsymbol{\mu}_{\boldsymbol{z} \mid j}, \boldsymbol{\Sigma}_{\boldsymbol{z} \mid j}), \quad (32)$$

where $f_{\boldsymbol{X},\boldsymbol{Z}}(\boldsymbol{x}, \boldsymbol{z}|\boldsymbol{\mu}_{\boldsymbol{z}|j},\boldsymbol{\Sigma}_{\boldsymbol{z}|j})$ is the joint PDF of $\boldsymbol{x}$ and $\boldsymbol{z}$ based on the j^{th} GMM component of $\boldsymbol{z}$'s PDF. Multiplying both the numerator and denominator in (30) by $g(\boldsymbol{z}|\boldsymbol{\mu}_{\boldsymbol{z}|i},\boldsymbol{\Sigma}_{\boldsymbol{z}|i})$, we can obtain the following formula,

$$f_{\boldsymbol{X} \mid \boldsymbol{Z}}(\boldsymbol{x} \mid \boldsymbol{z}) = \sum_{j=1}^{L_{\boldsymbol{z}}} \omega_{\boldsymbol{z} \mid j} \frac{g(\boldsymbol{z} \mid \boldsymbol{\mu}_{\boldsymbol{z} \mid j}, \boldsymbol{\Sigma}_{\boldsymbol{z} \mid j})}{f_{\boldsymbol{Z}}(\boldsymbol{z})} \frac{f_{\boldsymbol{X},\boldsymbol{Z}}(\boldsymbol{x},\boldsymbol{z} \mid \boldsymbol{\mu}_{\boldsymbol{z} \mid j}, \boldsymbol{\Sigma}_{\boldsymbol{z} \mid j})}{g(\boldsymbol{z} \mid \boldsymbol{\mu}_{\boldsymbol{z} \mid j}, \boldsymbol{\Sigma}_{\boldsymbol{z} \mid j})}. \quad (33)$$

Finally, integrating $\boldsymbol{x} f_{\boldsymbol{X}|\boldsymbol{Z}}(\boldsymbol{x}|\boldsymbol{z})$ with respect to $\boldsymbol{x}$ and using Proposition 2, the formula in (28) can be obtained. Therefore, IE($\boldsymbol{x}|\boldsymbol{z}$) in (28) presents the general formula of the proposed MMSE-based estimator, $\hat{\boldsymbol{x}}_{\text{MS}}$, as originally expressed in (13).

V. Properties of mean squared estimator

The purpose behind this section is to analyze the main properties of the proposed estimator, which are described below.

A. Umbiasedeness and minimum variance

Property 1 (Unbiasedness)—The estimator $\hat{\boldsymbol{x}}_{\text{MS}}$ as defined in (13) is unbiased.

Proof: It is obvious that $\hat{\boldsymbol{x}}_{\text{MS}} = \text{IE}(\boldsymbol{x}|\boldsymbol{z})$ is unbiased when $\boldsymbol{z}$ is GRV. By applying the mean function on both sides of the equation in (15), we can show,

$$\mathrm{IE}(\hat{\boldsymbol{x}}_{\mathrm{MS}}) = \boldsymbol{\mu}_{\boldsymbol{x}}. \quad (34)$$

For z being an NGRV, the expected value of the expression in (28) can be shown as,

$$\begin{aligned} &\mathrm{IE}\left(\frac{g(z \mid \boldsymbol{\mu}_{z \mid i}, \boldsymbol{\Sigma}_{z \mid i})}{f_{\boldsymbol{Z}}(z)}\left[z - \boldsymbol{\mu}_{z \mid i}\right]\right) \quad (35)\\ &= \int_{-\infty}^{\infty} \frac{g(z \mid \boldsymbol{\mu}_{z \mid i}, \boldsymbol{\Sigma}_{z \mid i})}{f_{\boldsymbol{Z}}(z)}\left[z - \boldsymbol{\mu}_{z \mid i}\right] f_{\boldsymbol{Z}}(z)\boldsymbol{dz}\\ &= \int_{-\infty}^{\infty} g(z \mid \boldsymbol{\mu}_{z \mid i}, \boldsymbol{\Sigma}_{z \mid i})\left[z - \boldsymbol{\mu}_{z \mid i}\right]\boldsymbol{dz}\\ &= 0. \end{aligned}$$

Therefore, applying the expectation function on all the elements of the summation in (28), the equation (34) is obtained which verifies that $\hat{\boldsymbol{x}}_{\mathrm{MS}}$ is an unbiased estimator.

Property 2 (Minimum variance)—an estimator is said to be a minimum variance estimator (MVE) if it has the smallest error variance [44].

Proof: Since this is a minimum mean squared error estimator [44], it is therefore an MVE. Moreover, the value of the error variance is given in (14).

Moreover, the minimum error variance that minimize the function in (12) as expressed in (14) can be further developed as,

$$\begin{aligned} J^{*}(\widetilde{\boldsymbol{x}}_{\mathrm{MS}}) &= \mathrm{IE}\left(\sum_{n \in \mathcal{N}} x_n^2 \mid z\right) - \sum_{n \in \mathcal{N}} (\mathrm{IE}(x_n \mid z))^2 \quad (36)\\ &= \sum_{n \in \mathcal{N}} \left(\mathrm{IE}(\boldsymbol{x}_n^2 \mid z) - (\mathrm{IE}(x_n \mid z))^2\right)\\ &= \sum_{n \in \mathcal{N}} \sigma^2(x_n \mid z_1, \ldots, z_M) \end{aligned}$$

Or,

$$\sigma^2(x_n \mid z_1, \ldots, z_M) \leq \sigma^2(x_n \mid z_1, \ldots, z_{j-1}, z_{j+1}, \ldots, z_M), \forall n \in \{1, \ldots, N\}, \forall j \in \{1, \ldots, M\} \quad (37)$$

Where M is the maximum number of PMU measurements based on full network observability. For instance, since the error is a zero-mean, the impact of missing a single measurement, e.g., z_j in (37), can be quantified by a positive added value to the minimum error variance as,

$$\Delta J^* = \sum_{n \in \mathcal{N}} \left(\sigma^2(x_n \mid z_1, \ldots, z_{j-1}, z_{j+1}) - \sigma^2(x_n \mid z_1, \ldots, z_M) \right). \quad (38)$$

Therefore, the maximum value of the minimum error variance can be reached in the absence of any measurements. This can be quantified as,

$$J^*(\widetilde{\boldsymbol{x}}_{\mathrm{MS}}) \leq J^*_{\max} = \sum_{n \in \mathcal{N}} \sigma^2_{x_n}. \quad (39)$$

It should be noted that the minimum required number of measurements depends on the statistics of the state parameters, as well as the selection of a suitable threshold value that we have imposed on the error variance. The threshold value is selected in order to provide a tradeoff between the state estimation accuracy and the number of measurements. This will be further discussed in the next section (i.e., see also Eq. 47).

B. Bad measurement identification

Many factors can lead to bad or corrupt measurements such as device malfunction or malicious data injection [48], [49]. The presence of bad measurements can be quantified by [50],

$$\boldsymbol{z}' = \boldsymbol{z} + \boldsymbol{o} \quad (40)$$

where $\boldsymbol{z}$ is as defined in (6) and $\boldsymbol{z}'$ is the infected measurements by an unknown vector $\boldsymbol{o}$. An element o_j in $\boldsymbol{o}$ is non-zero only if z_j is a bad datum. Therefore, using the general formula of MSE as given in (28), the impact of bad measurements on the estimated states can be expressed as,

$$\Delta \hat{\boldsymbol{x}}_{\mathrm{MS}} = \boldsymbol{B}\boldsymbol{o}. \quad (41)$$

with,

$$\boldsymbol{B} = \sum_{i=1}^{L_x} \sum_{j=1}^{L_z} \omega_{\boldsymbol{x} \mid i} \omega_{\boldsymbol{z} \mid i} A_{\boldsymbol{x} \mid i, \boldsymbol{z} \mid j} \quad (42)$$

On the other hand, from (14) and using $\mathrm{IE}(\boldsymbol{x}|\boldsymbol{z}) = \hat{\boldsymbol{x}}_{MS}$, we obtain,

$$J^*(\widetilde{\boldsymbol{x}}_{\mathrm{MS}}) = \mathrm{IE}(\boldsymbol{x}^{\mathrm{T}}\boldsymbol{x} \mid z) - \hat{\boldsymbol{x}}_{MS}^{T}\hat{\boldsymbol{x}}_{MS}. \quad (43)$$

Therefore, based on an proposition 3, $J^*(\widetilde{\boldsymbol{x}}_{\mathrm{MS}})$ can be calculated immediately using the GMM presentation of the PDF of $\boldsymbol{x}^{\mathrm{T}}\boldsymbol{x}$. Moreover, the mean value of $J^*(\widetilde{\boldsymbol{x}}_{\mathrm{MS}})$ can be evaluated using the following property of conditional variance,

$$\sigma_{\boldsymbol{x}}^2 = \mathrm{IE}(\sigma^2(\boldsymbol{x} \mid z)) + \sigma^2(\mathrm{IE}(\boldsymbol{x} \mid z)), \quad (44)$$

In other expression,

$$\mathrm{IE}(\sigma^2(\boldsymbol{x} \mid z)) = \sigma_{\boldsymbol{x}}^2 - \sigma_{\hat{\boldsymbol{x}}_{MS}}^2. \quad (45)$$

From (36) and (45),

$$\mathrm{IE}(J^*(\widetilde{\boldsymbol{x}}_{\mathrm{MS}})) = \sum_{n \in \mathcal{N}} \left(\sigma_{\boldsymbol{x}}^2 - \sigma_{\hat{\boldsymbol{x}}_{MS}}^2\right)_n. \quad (46)$$

where $(\sigma_{\boldsymbol{x}}^2 - \sigma_{\hat{\boldsymbol{x}}_{MS}}^2)_n$ is the n^{th} component of $\sigma_{\boldsymbol{x}}^2 - \sigma_{\hat{\boldsymbol{x}}_{MS}}^2$. Knowing the mean value of the minimum error variance in the case of no bad data present in the measurements vector, a threshold of $J^*(\widetilde{\boldsymbol{x}}_{\mathrm{MS}})$ can be defined in terms of $\mathrm{IE}(J^*(\widetilde{\boldsymbol{x}}_{\mathrm{MS}}))$ as,

$$J^*(\widetilde{\boldsymbol{x}}_{\mathrm{MS}}) \leq \alpha \mathrm{IE}(J^*(\widetilde{\boldsymbol{x}}_{\mathrm{MS}})) \quad (47)$$

This criteria allows to determine if the measurements vector is holding a bad datum. In the case of the minimum variance bigger than the threshold, it is proposed to eliminate one-by-one measurements and reevaluate until respect of the criteria.

VI. Simulation and discussions

Simulations using benchmark IEEE test networks i.e, IEEE 14-bus, IEEE 30-bus and IEEE 118-bus have been conducted to validate the performances of the MMSE-based approach for power systems. In this section, a description of our simulation environment and test systems are presented followed by a brief description of a benchmark estimation method such as WLS, which is used for the sake of comparison. Finally, we analyze and discuss the results.

A. Simulations description

Performances of the proposed MMSE-based estimator for the three test models are evaluated using the IEEE test models. Bear in mind that the proposed approach requires a prior probability of the SPF in order to provide distribution for both estimated and measured parameters. For the sake of generalization, we use the data provided in [51], [52] for power generation while the load power is assumed to be random variables with mean values equal to the load, as in [51], [52].We assume that all the loads have a ratio of the standard deviation over the mean value; $CV = 0.1$. To validate the performance of the proposed approach for a general case of non-Gaussian parameters, GMM parameters are required. For the sake of simplification and generalization, a data in the case of two Gaussian components is randomly generated given the mean and standard deviation of the power at each bus and verifying the GMM conditions in (4) and (5).

The active power at all the buses is assumed to be correlated. The correlation matrix for load powers is generated randomly in [0, 1] and is kept the same within the GMM components while the active and reactive powers are assumed to be fully correlated while keeping the power factor constant. Then the Monte Carlo simulations (MCS) are ran for $\mathcal{N}_{\text{mcs}} = 10000$ simulations in order to solve the Newton Raphson based power flow using the package of MATLAB *MATPOWER* provided in [53]. Based on the MCS results, the fitting function of Matlab "*gmdistribution.fit*" is then used to provide the GMM components of the MCS outputs; mainly the estimation parameters and the measurements. This function gives maximum likelihood estimates of the parameters in a Gaussian mixture model with, for instance, $k = 2$ components. The analytical formula of the proposed MSE estimator expresses the estimated parameters as the mean value corrected by an additive term which is the product of the covariance matrices of estimated and measured parameters and the subtraction of current value and mean value of the measurements (see equation (28)). This process would allow the estimator to perform a highly accurate state estimation with a limited number of measurements. To validate this capability, four different cases, defined by the number redundancy of the measurements as shown in Table I, have been investigated. Note that the redundancy is defined as the ratio of the measurements number over estimated parameters number [22]. The notations $|\mathcal{N}_s|$, $|\mathcal{Z}_{\theta,V}|$, $|\mathcal{Z}_{P,Q}|$ and $|\mathcal{Z}_{P_f Q_f}|$ are the sizes of the estimated parameters, the measured voltage, the measured power injection and measured power low sets respectively. We assume an Additive White Gaussian noise (AWGN) for the measurements with standard deviations of 1% for voltage (amplitude and angle) and 2% for power injections and flows. A sample size of $\mathcal{N}_{\text{spl}} = 200$ has been considered for the MCS running of WLS, UKF, and MSE. In these experiments we consider $\mathcal{N}_{\text{spl}}$ different measurements generated according to the obtained PDFs from the SPF study. For each

experiment, WLS, UKF, and MSE have been used to calculate the estimated states, i.e. voltage amplitude and angle. These simulations have been run on an Intel i7-4600U processor at 2.7 GHz using a Matlab code.

B. Comparison methods

In this study, WLS and UKF have been used as reference methods to evaluate the relative performance of the proposed MSE method, especially in the case of redundant measurements scenarios. Furthermore, for scenarios with a limited number of measurement where the is no guarantee that WLS and UKF can converge, we consider a combination of compressive sensing and UKS which will be referred to as CS-UKF. Such a combination is inspired by the SPF methods presented in [49], [50], [54], [55]. In this paper, a CSUKF-based approach is developed as an additional reference method to aid our evaluations. This method is based on two successive steps. The first considers CS to reconstruct the measurements vector followed by UKF to estimate the system states. The CS process exploits the available statistics on the measurement parameters, as well as their correlations to reconstruct the complete vector of measurements. Bear in mind that the CS theory is based on reconstruction of the complete signal (more redundant measurement vector) from available compressed measurements (less redundant measurements vector). The availability of statistics on the state parameters makes the measurement vector a spare signal which can then be compressed and reconstructed. The recovery of a more redundant measurement vector z^r from a limited measurement vector using the SPF information can be developed as,

$$\hat{z}^r = \mathrm{IE}(z^r \mid z^m) \quad (48)$$

where $\hat{z}^r$ is the recovered measurements vector. Therefore, using Proposition 3, the conditional expectation can be evaluated from the measurement parameters statics. Note that z^r contains z^m elements besides other unavailable measurements, then $|z^r| - |z^m|$.

C. Performance comparisons

In these experiments we compare the performance of the proposed MSE to those obtained by WLS and UKF. The true values are considered as the state values obtained from the power flow. To assess MSE, UKF and WLS performances, the mean absolute error ($\hat{x}_{\mathrm{MAE}}$) of both voltage amplitude and angle are calculated using the following expression,

$$\hat{x}_{\mathrm{MAE}} = \frac{1}{\mathcal{N}_x} \sum_{i=1}^{\mathcal{N}_x} \mathrm{IE}_{\mathrm{spl}}(\mid \hat{x}_i - x_i^{true} \mid), \quad (49)$$

with

$$\mathrm{IE}_{\mathrm{spl}}(x) = \frac{1}{\mathcal{N}_{spl}} \sum_{j=1}^{N_{spl}} x_j$$

where x_j is the value of x corresponding to the j^{th} element in the considered sample. x_i^{true} and $\hat{x}_I$ are the true and estimated values of state i, while $\mathcal{N}_x$ is the number of estimated states.

D. Results and discussion

Table II displays the $\hat{V}_{\mathrm{MAE}}$ and $\hat{\theta}_{\mathrm{MAE}}$ results for the IEEE test models using 4 different numbers of measurements (i.e., case 1–4). For the three test system, WLS converges for cases 1 and 2. However, it diverges for cases 3 and 4 where the measurement redundancy is lower (<≃ 1). Comparing cases 1 and 2, the results show that MSE outperforms WLS and UKF in terms of MAE values (see equation 49). Fig. 1 illustrates the values of mean absolute error over the considered sample of each estimated state. Figs. 1a, 1b and 1c show the voltage amplitudes absolute error for IEEE-14, -30 and -118 bus, respectively, while Figs. 1d, 1e and 1f display their voltage angles absolute error. As can be observed for all three IEEE test models, the MSE performances are well below those of WLS and UKF for all buses verifying the superior performances of the proposed estimator. In addition, with an even smaller number of measurements (e.g., cases 3 and 4), the performance of MSE does not deteriorate considerably as indicated in Table II. Fig. 2 illustrates the obtained curves of the mean absolute error over the considered simulation sample of each estimated state. Indeed, Figs. 2a, 2b and 2c illustrate the voltage amplitudes absolute error for IEEE-14, -30 and -118 bus respectively. Moreover, Figs. 2d, 2e and 2f are illustrating voltage angles absolute error for IEEE-14, -30 and -118 bus respectively. Finally, for the sake of comparison in cases 3 and 4 where WLS and UKF do not converge, CS-UKF has been deployed and the results are illustrated in Fig. 3. It shows that MSE overcomes CS-UKF. Besides, comparing the execution time of the estimation methods which are given in Table II, which shows that MSE can significantly outperform CS-UKF. In addition, as shown in Table II, CSUKF, UKF and WLS, due to their iterative nature, would require a significantly higher execution time than MSE. This unique future is important for real-time grid monitoring and fast state estimation.

E. Case of bad measurements

The study of this case aims at showing the performances of the proposed estimator on identifying and eliminating bad measured data. To realize this purpose, a samples of 200 estimations is evaluated using MSE. In this case, arbitrary values have been added to the measurement vector at iterations over the range [50–59] to one parameter and over [100–109] to two parameters applied to IEEE-118 bus network. Fig. 4 illustrates the variation of the voltage angle estimation. It is shown in Fig. 4a that the error increases clearly when some measurements are corrupted. Moreover, as expected in our previous analysis, the error variance also increases in terms of number and value of the bad datum which allows to identify and then eliminate it. To decide whether the measurements are corrupted or not, a chosen value of $\alpha = 2$ in the criteria in (47).

F. Use case using EMTP-RV

The design of the proposed estimator is based on availability of the system statistics under various test environments. To gather such statistics we use an EMTP-RV [1] software tool for real-time assessment of the proposed method [56]. EMTP-RV is an Electro Magnetic Transients Program (EMTP) software tool where PMU devices can be placed at any desirable location in the grid network. EMTP-RV has been widely used as a time domain transient solution [24], [57]. It is able to provide almost all power system components, such as power plant, transformer, windfarm, different kinds of faults, overhead lines with line and ground wires and towers, as well as underground cables. In our experiments using EMTP-RV we considered the IEEE 39-bus transmission model where PMUs are placed on buses to collect and process samples of power signals. To assess the impact of uncertainties on the proposed state estimation, we added 4 wind parks, each of 100 wind turbines of 1.5MW, and 4 photovoltaic farms, each of 34 solar arrays of 2MW to the IEEE 39-bus, as illustrated in Fig. 6. Power and voltage signals generated by EMTP-RV have been collected and then applied to evaluate the MSE performance. Fig. 5 illustrates the mean absolute error for the 4 measurement configurations given in Table I.

VII. Conclusion

In this paper, a new analytical-based state estimator, referred to as Mean Squared Estimator (MSE), has been proposed for the general case where a state parameters and measurements are non-Gaussian random variables (NGRV's). In our analysis, we use the GMM to approximate the NGRV's PDF as a weighted summation of Gaussian components to derive a general formula as a conditional expectation of the estimated states for a given set of measurements. Simulations have been carried out using three benchmark IEEE test models. The performance of the proposed MSE approach has been compared to those of WLS, UKF and CS-UKF. The results verify that the proposed approach outperforms the background methods. It is also shown that the proposed state estimator can perform highly accurate estimations with a limited number of measurements. This work will be extended in order to present more analysis on dynamic SPF and on the sensitivity of SPF error on the MSE results.

References

1. Zhang P, Lee ST. Probabilistic Load Flow Computation Using the Method of Combined Cumulants and Gram-Charlier Expansion. IEEE Transactions on Power Systems. 19(1):676–682.2004;
2. Morales JM, Pérez-Ruiz J. Point estimate schemes to solve the probabilistic power flow. IEEE Transactions on Power Systems. 22(4):1594–1601.2007;
3. Bazrafshan M, Gatsis N. Decentralized stochastic optimal power flow in radial networks with distributed generation. IEEE Transactions on Smart Grid. PP(99):1–15.2016;
4. Peng S, Tang J, Li W. Probabilistic Power Flow for AC/VSC-MTDC Hybrid Grids Considering Rank Correlation among Diverse Uncertainty Sources. IEEE Transactions on Power Systems. 8950(c):1–1.2017;

[1]Certain commercial equipment, instruments, or materials are identified in this paper to foster understanding. Such identification does not imply recommendation or endorsement by the National Institute of Standards and Technology, nor does it imply that the materials or equipment identified are necessarily the best available for the purpose.

5. Mohammadi M, Basirat H, Kargarian A. Nonparametric Probabilistic Load Flow with Saddle Point Approximation. IEEE Transactions on Smart Grid. 3053(c):1–1.2017;
6. Nijhuis M, Gibescu M, Cobben JFG. Gaussian Mixture Based Probabilistic Load Flow for LV-Network Planning. IEEE Transactions on Power Systems. 8950(c):1–1.2016;
7. Prusty BR, Jena D. Combined cumulant and Gaussian mixture approximation for correlated probabilistic load flow studies: a new approach. CSEE Journal of Power and Energy Systems. 2(2): 71–78.2016;
8. Valverde G, Saric AT, Terzija V. Stochastic monitoring of distribution networks including correlated input variables. IEEE Transactions on Power Systems. 28(1):246–255.2013;
9. Ren Z, Li W, Billinton R, Yan W. Probabilistic Power Flow Analysis Based on the Stochastic Response Surface Method. 31(3):2307–2315.2016;
10. Dash P. Two-Level Dynamic Stochastic Optimal Power Flow Control for Power Systems With Intermittent Renewable Generation. IEEE Transactions on Power Systems. 28(3):2670–2678.2013;
11. Fan M, Vittal V, Heydt GT, Ayyanar R. Probabilistic power flow studies for transmission systems with photovoltaic generation using cumulants. IEEE Transactions on Power Systems. 27(4):2251–2261.2012;
12. Ahmed MH, Bhattacharya K, Salama MMA. Probabilistic distribution load flow with different wind turbine models. IEEE Transactions on Power Systems. 28(2):1540–1549.2013;
13. Aien M, Fotuhi-Firuzabad M, Aminifar F. Probabilistic load flow in correlated uncertain environment using unscented transformation. IEEE Transactions on Power Systems. 27(4):2233–2241.2012;
14. Guo Z, Li S, Wang X, Heng W. Distributed Point-Based Gaussian Approximation Filtering for Forecasting-Aided State Estimation in Power Systems. IEEE Transactions on Power Systems. 31(4):2597–2608.2016;
15. Shih K, Huang S. Application of a robust algorithm for dynamic state estimation of a power system. Power Systems, IEEE Transactions on. 17(1):141–147.2002;
16. Lin J, Huang S, Shih K. Application of sliding surface-enhanced fuzzy control for dynamic state estimation of a power system. Power Systems, IEEE. 18(2):570–577.2003;
17. Wang S, Gao W, Meliopoulos APS. An alternative method for power system dynamic state estimation based on unscented transform. IEEE Transactions on Power Systems. 27(2):942–950.2012;
18. Huang SJ, Lin JM. Enhancement of Anomalous Data Mining in Power System Predicting-Aided State Estimation. IEEE Transactions on Power Systems. 19(1):610–619.2004;
19. Cao X, Stephen B, Abdulhadi IF, Booth CD, Burt GM. Switching Markov Gaussian Models for Dynamic Power System Inertia Estimation. IEEE Transactions on Power Systems. 31(5):3394–3403.2016;
20. Rouhani A, Member IS, Abur A. Observability Analysis for Dynamic State Estimation of Synchronous Machines. 8950(c):1–8.2016;
21. Gu C, Jirutitijaroen P. Dynamic State Estimation Under Communication Failure Using Kriging Based Bus Load Forecasting. IEEE Transactions on Power Systems. 30(6):2831–2840.2015;
22. Zhao J, Zhang G, Dong ZY, La Scala M. Robust Forecasting Aided Power System State Estimation Considering State Correlations. IEEE Transactions on Smart Grid. 3053(c):1–1.2016;
23. Zhao J, Netto M, Mili L. A Robust Iterated Extended Kalman Filter for Power System Dynamic State Estimation. IEEE Transactions on Power Systems. 8950(c):1–1.2016;
24. Gharavi H, Hu B. Space-Time Approach for Disturbance Detection and Classification. IEEE Transactions on Smart Grid. :1–1.2017
25. Gharavi H, Hu B. Scalable Synchrophasors Communication Network Design and Implementation for Real-Time Distributed Generation Grid. IEEE Transactions on Smart Grid. 6(5):2539–2550.2015;
26. Ghahremani E, Kamwa I. Local and wide-area PMU-based decentralized dynamic state estimation in multi-machine power systems. IEEE Transactions on Power Systems. 31(1):547–562.2016;

27. Yu S, Member S, Fernando T, Member S, Emami K, Iu HH-c, Member S. Dynamic State Estimation Based Control Strategy for DFIG Wind Turbine Connected to Complex Power Systems. 32(2):1272–1281.2017;
28. Singh AK, Pal BC. Decentralized Dynamic State Estimation in Power Systems Using Unscented Transformation. 29(2):794–804.2014;
29. Sarri S, Zanni L, Popovic M, Le Boudec JY, Paolone M. Performance Assessment of Linear State Estimators Using Synchrophasor Measurements. IEEE Transactions on Instrumentation and Measurement. 65(3):535–548.2016;
30. Bian X, Li XR, Chen H, Gan D, Qiu J. Joint Estimation of State and Parameter With Synchrophasors #x2014;Part II: Parameter Tracking. Power Systems, IEEE Transactions on. 26(3): 1209–1220.2011;
31. Ashton PM, Taylor GA, Irving MR, Pisica I, Carter AM, Bradley ME. Novel application of detrended fluctuation analysis for state estimation using synchrophasor measurements. IEEE Transactions on Power Systems. 28(2):1930–1938.2013;
32. Yang P, Tan Z, Wiesel A, Nehorai A. Power system state estimation using PMUs with imperfect synchronization. IEEE Transactions on Power Systems. 28(4):4162–4172.2013;
33. Milton Brown Do Coutto Filho J. Forecasting-Aided State Estimation-Part I: Panorama Milton. IEEE Transactions on Power Systems. 24(4):1667–1677.2009;
34. Milton Brown Do Coutto Filho J. Forecasting-Aided State Estimation Part II : Implementation. 24(4):1678–1685.2009;
35. Sharma A, Srivastava SC, Chakrabarti S. Testing and Validation of Power System Dynamic State Estimators Using Real Time Digital Simulator (RTDS). IEEE Transaction on Power System. 31(3):2338–2347.2016;
36. Ghahremani E, Kamwa I. Dynamic State Estimation in Power System by Applying the Extended Kalman Filter With Unknown Inputs to Phasor Measurements. Power Systems, IEEE Transactions on. 26(4):2556–2566.2011;
37. Lee G, Scott C. EM algorithms for multivariate Gaussian mixture models with truncated and censored data. Computational Statistics and Data Analysis. 56(9):2816–2829.2012;
38. Manitsas E, Singh R, Pal BC, Strbac G. Distribution system state estimation using an artificial neural network approach for pseudo measurement modeling. IEEE Transactions on Power Systems. 27(4):1888–1896.2012;
39. Ke D, Chung CY, Sun Y. A novel probabilistic optimal power flow model with uncertain wind power generation described by customized Gaussian mixture model. IEEE Transactions on Sustainable Energy. 7(1):200–212.2016;
40. Gemine, Q; Corn, B; Glavic, M; Fonteneau, R; Ernst, D. A Gaussian mixture approach to model stochastic processes in power systems. Power Systems Computation Conference (PSCC); 2016; 2016.
41. Cui M, Feng C, Wang Z, Zhang J. Statistical Representation of Wind Power Ramps Using a Generalized Gaussian Mixture Model. IEEE Transactions on Sustainable Energy. 3029(c):1–12.2017;
42. Valverde G, Saric A, Terzija V. Probabilistic load flow with non-Gaussian correlated random variables using Gaussian mixture models. IET Generation, Transmission & Distribution. 6(7): 701.2012;
43. Valverde G, Saric aT, Terzija V. Probabilistic load flow with non-Gaussian correlated random variables using Gaussian mixture models. IET Generation, Transmission & Distribution. 6(7): 701.2012;
44. Mendel, JM. Lessons in Estimation Theory for Signal Processing, Communications, and Control. In: Oppenheim, Alan V, editor. Prentice Hall Signal Processing Series. 1995.
45. Abur, A, Exposito, A. Power system state estimation: theory and implementation. Marcel Dekker, Inc; Cimarron Road, Monticello, New York 12701, U.S.A: 2004.
46. Shiryaev, AN. U. Sheldon Axler San Francisco State University, San Francisco, CA, U. Kenneth Ribet University of California, Berkeley, CA, and Advisory. Probability-1. 3. Vol. 95. Springer; 2016.

47. Papoulis, APIoNY. S. C.-M. U. w. Director. Probability, Random Variables, and Stochastic Processes. 3. New York: McGraw-Hill Series in Electrical Engineering; 1991.
48. Kosut O, Jia L, Thomas RJ, Tong L. Malicious data attacks on the smart grid. IEEE Transactions on Smart Grid. 2(4):645–658.2011;
49. Kekatos V, Giannakis GB. Distributed robust power system state estimation. IEEE Transactions on Power Systems. 28(2):1617–1626.2013;
50. Kekatos V, Giannakis GB. From Sparse Signals to Sparse Residuals for Robust Sensing. IEEE Transactions on Power Systems. 59(7):3355–3368.2011;
51. Christie, RD. Power Systems Test Case Archive. 1999. [Online]. Available: http://www2.ee.washington.edu/research/pstca/
52. Bila, C. PhD dissertation. Northeastern University; Boston, Massachusetts: 2013. POWER SYSTEM DYNAMIC STATE ESTIMATION and LOAD MODELING.
53. Ray, DZ; Carlos, EM-S; , et al. A MATLAB Power System Simulation Package. [Online]. Available: http://www.pserc.cornell.edu/matpower/
54. Alam SMS, Natarajan B, Anil P. Distribution Grid State Estimation from Compressed Measurements. IEEE Transactions on Smart Grid. 5(4):1631–1642.2014;
55. Majidi M, Etezadi-Amoli M, Livani H. Distribution system state estimation using compressive sensing. International Journal of Electrical Power and Energy Systems. 88:175–186.2017;
56. Gharavi H, Hu B. Synchrophasor Sensor Networks for Grid Communication and Protection. Proceedings of the IEEE. 105(7):1408–1428.2017; [PubMed: 28890553]
57. Dommel H. Digital Computer Solution of Electromagnetic Transients in Single-and Multiphase Networks. IEEE Transactions on Power Apparatus and Systems. PAS-88(4):388–399.1969;

Biographies

Hasnae Bilil (S'11-M'15) received the Dipl.-Ing in 2010 and the Ph.D. degree in 2014 in electrical engineering from Mohammadia School of Engineers (EMI), Rabat, Morocco. She joined EMI as a teaching assistant from 2011 until 2015. Since August 2015, she is conducting research on smart grids and renewable energy integration as a Post-Doc at National Institute of Standards and Technology. Her current research interests include renewable energy sources, power system state estimation, smart grid and demand side management.

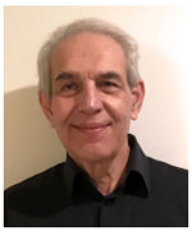

HAMID GHARAVI received his Ph.D. degree from Loughborough University, United Kingdom, in 1980. He joined the Visual Communication Research Department at AT&T

Bell Laboratories, Holmdel, New Jersey, in 1982. He was then transferred to Bell Communications Research (Bellcore) after the AT&T-Bell divestiture, where he became a consultant on video technology and a Distinguished Member of Research Staff. In 1993, he joined Loughborough University as a professor and chair of communication engineering. Since September 1998, he has been with the National Institute of Standards and Technology (NIST), U.S. Department of Commerce, Gaithersburg, Maryland. He was a core member of Study Group XV (Specialist Group on Coding for Visual Telephony) of the International Communications Standardization Body CCITT (ITUT). His research interests include smart grid, wireless multimedia, mobile communications and wireless systems, mobile ad hoc networks, and visual communications. He holds eight U.S. patents and has over 150 publications related to these topics. He received the Charles Babbage Premium Award from the Institute of Electronics and Radio Engineering in 1986, and the IEEE CAS Society Darlington Best Paper Award in 1989. He was the recipient of the Washington Academy of Science Distinguished Career in Science Award for 2017. He served as a Distinguished Lecturer of the IEEE Communication Society. He has been a Guest Editor for a number of special issues of the Proceedings of the IEEE, including Smart Grid, Sensor Networks & Applications, Wireless Multimedia Communications, Advanced Automobile Technologies, and Grid Resilience. He was a TPC Co-Chair for IEEE SmartGridComm in 2010 and 2012. He served as a member of the Editorial Board of Proceedings of the IEEE from January 2003 to December 2008. From January 2010 to December 2013 he served as Editor-in-Chief of IEEE Transactions on CAS for Video Technology. He is currently serving as the Editor-in-Chief of IEEE Wireless Communications.

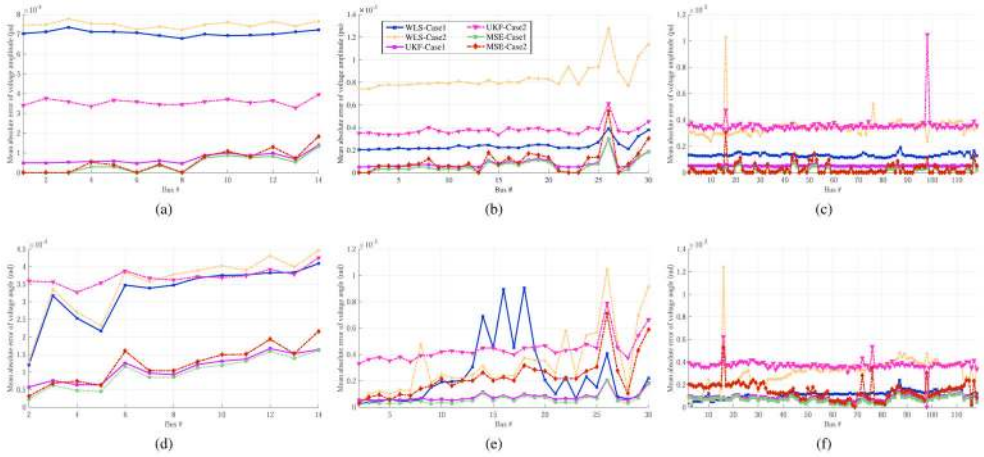

Fig. 1.

Comparison of $\mathrm{IE}_{\mathrm{spl}}(\mid \hat{V}_i - V_i^{true} \mid)$ for (a) IEEE-14 bus, (b) IEEE-30 bus and (c) IEEE-118 bus and of $\mathrm{IE}_{\mathrm{spl}}(\mid \hat{\theta}_i - \theta_i^{true} \mid)$ for (d) IEEE-14 bus, (e) IEEE-30 bus and (f) IEEE-118 bus using WLS, UKF and MSE in cases 1 and 2 of measurements configuration.

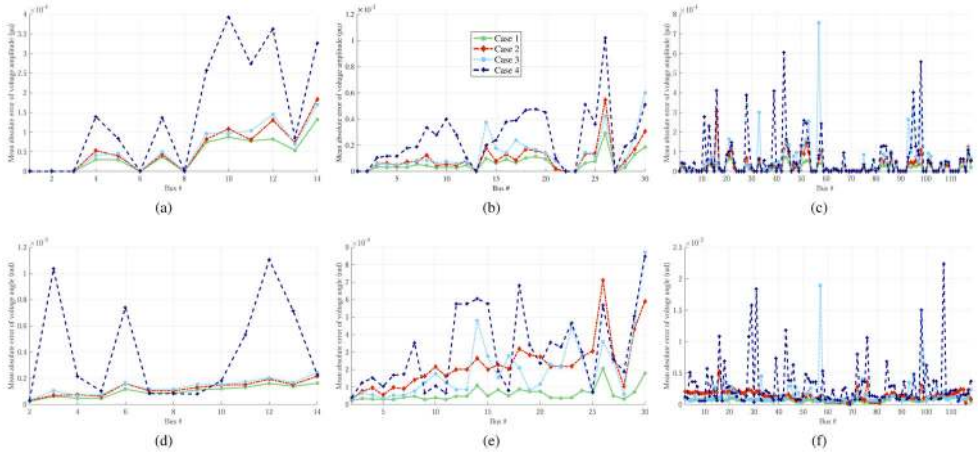

Fig. 2.

Comparison of $\mathrm{IE}_{\mathrm{spl}}(\,|\,\hat{V}_i - V_i^{true}\,|\,)$ for (a) IEEE-14 bus, (b) IEEE-30 bus and (c) IEEE-118 bus and of $\mathrm{IE}_{\mathrm{spl}}(\,|\,\hat{\theta}_i - \theta_i^{true}\,|\,)$ for (d) IEEE-14 bus, (e) IEEE-30 bus and (f) IEEE-118 bus using MSE in cases 1, 2, 3 and 4 of measurements configuration.

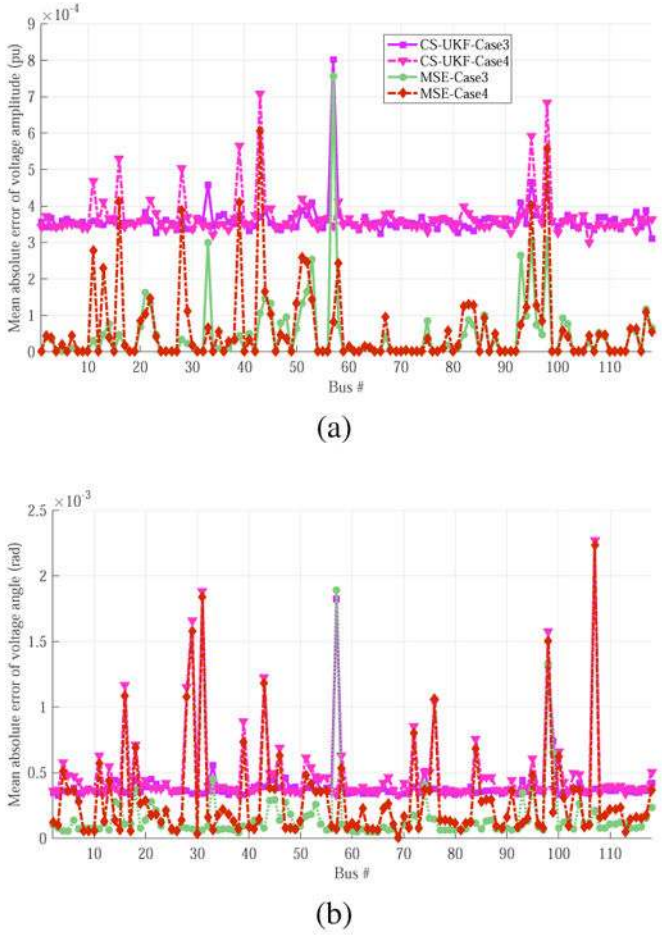

Fig. 3.

Comparison of (a) $IE_{spl}(|\hat{V}_i - V_i^{true}|)$ and of (b) $IE_{spl}(|\hat{\theta}_i - \theta_i^{true}|)$ for IEEE-118 bus using CS-UKF and MSE in cases 3 and 4 of measurements configuration.

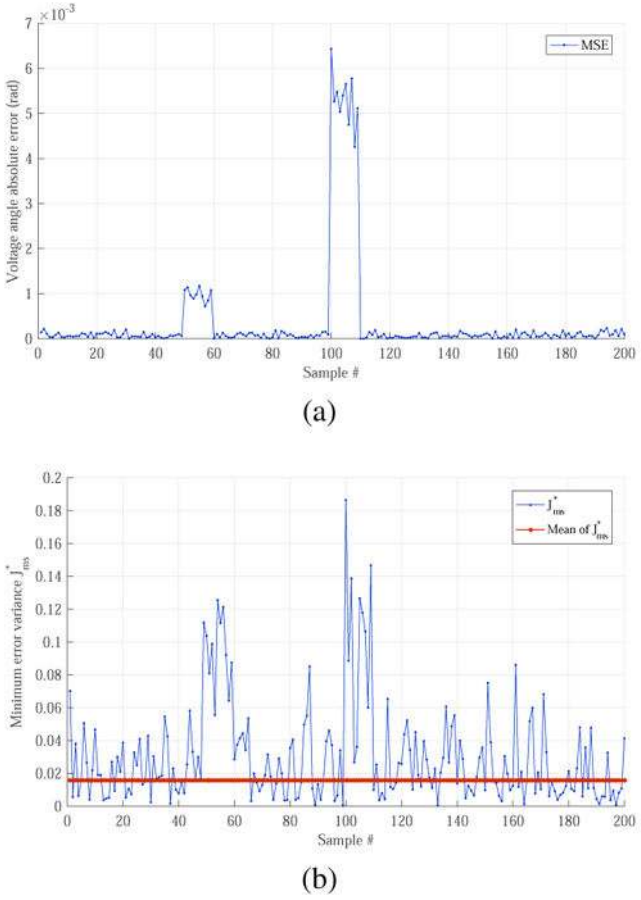

Fig. 4.

Illustration of (a) $\mathrm{IE}_{\mathrm{spl}}(|\hat{\theta}_i - \theta_i^{true}|)$ and (b) its corresponding minimum error variance for IEEE-118 bus in the case of bad datum.

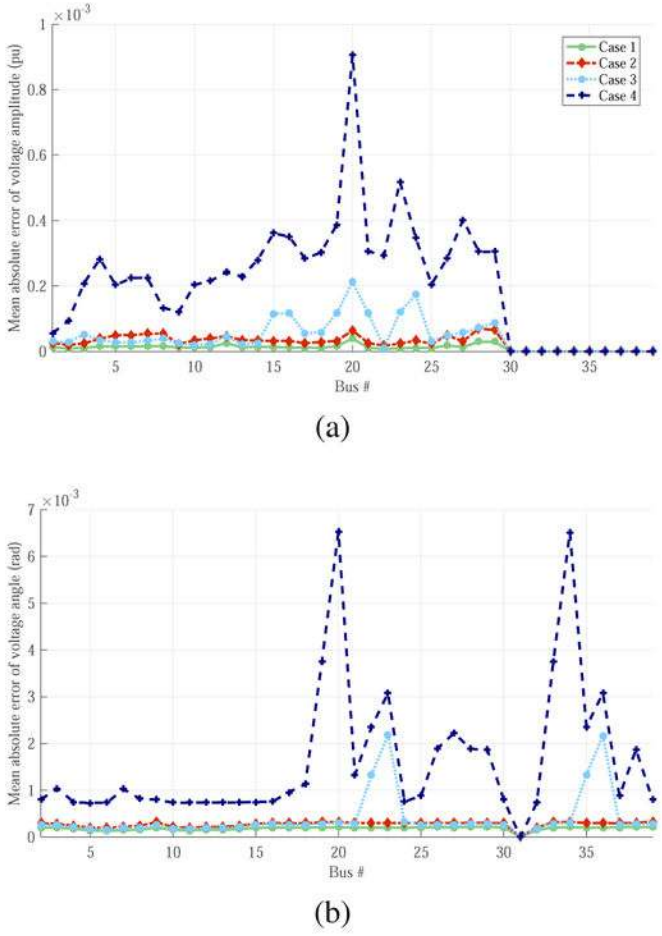

Fig. 5.

Comparison of (a) $IE_{spl}(|\hat{V}_i - V_i^{true}|)$ and of (b) $IE_{spl}(|\hat{\theta}_i - \theta_i^{true}|)$ for IEEE-118 bus using MSE in cases 1, 2, 3 and 4 of measurements configuration.

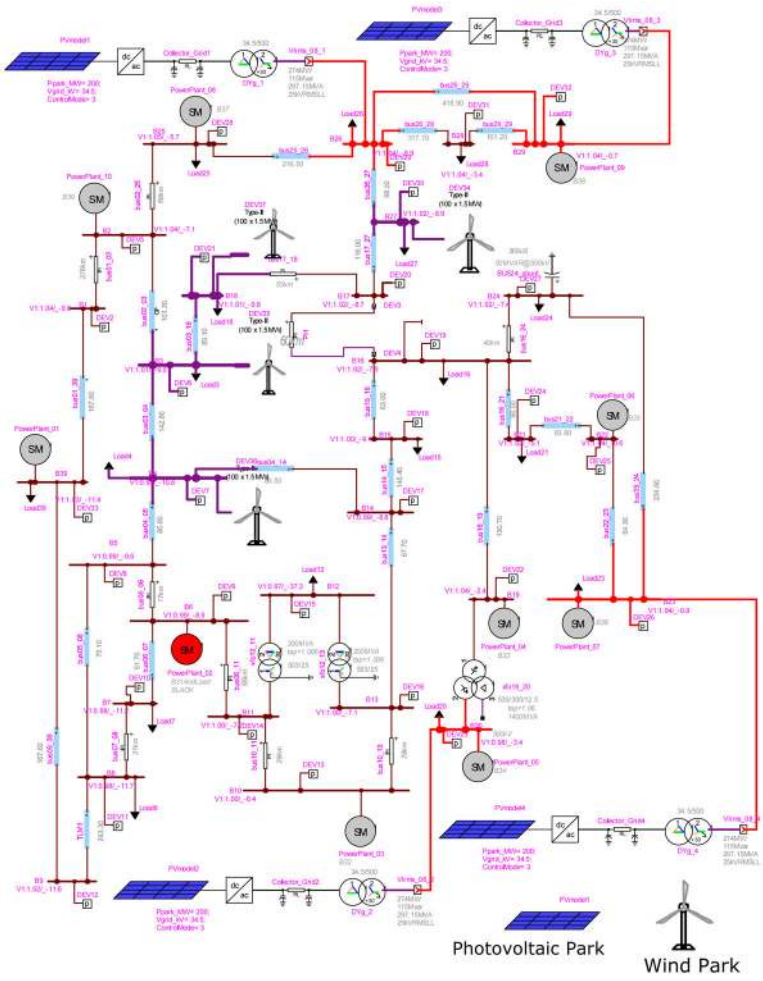

Fig. 6.
IEEE 39–bus with high penetration of distributed generation

TABLE I

Measurements configuration for the 3 test networks

Test system	Case	$\lvert\mathcal{N}_s\rvert$	$\lvert\mathcal{Z}_{\theta,V}\rvert$	$\lvert\mathcal{Z}_{P,Q}\rvert$	$\lvert\mathcal{Z}_{P_f,Q_f}\rvert$	Redundancy
IEEE 14-bus	1	27	14	28	40	3.04
	2	27	8	14	20	1.56
	3	27	4	10	14	1.04
	4	27	4	8	10	0.81
IEEE 30-bus	1	59	30	60	82	2.90
	2	59	16	30	42	1.50
	3	59	10	20	28	0.98
	4	59	8	16	22	0.78
IEEE 118-bus	1	235	118	236	372	3.09
	2	235	60	118	186	1.55
	3	235	40	78	124	1.03
	4	235	30	60	94	0.78
IEEE 39-bus	1	77	40	80	110	2.99
	2	77	20	40	56	1.51
	3	77	14	26	38	1.01
	4	77	10	20	28	0.75

TABLE II

Mean values of the absolute error for different measurements configuration of IEEE benchmark systems

Test system	$\hat{V}_{MAE} \times 10^3$					$\hat{\theta}_{MAE} \times 10^3$					Execution time (ms)
	Method	Cases				Method	Cases				
		1	2	3	4		1	2	3	4	
IEEE 14-bus	WLS	0.7060	0.8065	NA	NA	WLS	0.3228	0.3937	NA	NA	210
	UKF	0.0719	0.3581	NA	NA	UKF	0.1117	0.3703	NA	NA	3141
	CS-UKF	0.0719	0.0891	0.3440	0.3491	CS-UKF	0.1117	0.2633	0.3638	0.8483	3150
	MSE	0.0422	0.0606	0.1652	0.1516	MSE	0.1046	0.1292	0.1843	0.4783	7
IEEE 30-bus	WLS	0.2394	0.8950	NA	NA	WLS	0.2423	0.3054	NA	NA	65
	UKF	0.0839	0.3755	NA	NA	UKF	0.0779	0.4419	NA	NA	815
	CS-UKF	0.0839	0.1235	0.3839	0.7295	CS-UKF	0.0779	0.1015	0.2993	0.5043	823
	MSE	0.0595	0.0995	0.1262	0.2549	MSE	0.0600	0.2292	0.1993	0.3139	8
IEEE 118-bus	WLS	0.1324	0.3892	NA	NA	WLS	0.1125	0.5717	NA	NA	569
	UKF	0.0540	0.3575	NA	NA	UKF	0.0843	0.3967	NA	NA	9298
	CS-UKF	0.0540	0.0983	0.3501	0.3532	CS-UKF	0.0843	0.0523	0.3508	0.3499	9324
	MSE	0.0147	0.0361	0.0465	0.0626	MSE	0.0668	0.1674	0.1504	0.2993	26